

Comparison between two methods for monitoring deformation with Laser Scanner

VINCENZO BARRILE (*), GIUSEPPE M. MEDURI (*), GIULIANA BILOTTA (**)

* DICEAM - Faculty of Engineering

“Mediterranea” University of Reggio Calabria

Via Graziella Feo di Vito 89100 Reggio Calabria, Tel +39 0965 875301

** Ph.D. NT&ITA – Dept. of Planning - University IUAV of Venice

Santa Croce 191, Tolentini 30135 Venice

ITALY

vincenzo.barrile@unirc.it, giumed@libero.it, giuliana.bilotta@gmail.com

Abstract: - This contribute describes two methods for monitoring and control of mountain areas with Terrestrial Laser Scanner using laser scans performed in two time periods, and having as aim the study of possible deformations. In the first method, the registration of scans at each epoch was made using the algorithm ICP (Iterative Closest Point) while the generation of the DEM for analysis of the Δ DEM differences between the two epochs was made with the RANSAC (RANDOM SAMPLE CONSENSUS) algorithm.

With the second method, the registration of the point cloud for each period and then the estimation of displacement took place with a procedure based on the algorithm “Least squares 3D surface matching” without the need to use the target scans and DEM generation.

Key-Words: - Laser Scanner - ICP algorithm – DEM - RANSAC algorithm - Least squares 3D surface matching

1 Introduction and study area

The Faculty of Agriculture of the University “Mediterranea” of Reggio Calabria is built on a hill that offers a specific geomorphology. In fact, after the construction of the Faculty building have arisen some problems regarding its stability and possible deformations also because of poor vegetation.

The Laboratory of Geomatics Engineering Faculty of the University “Mediterranea” of Reggio Calabria used terrestrial laser scanner for monitoring the hill (Fig.1) doing the scans after three years and examining the results obtained. Every era we made two scans, that we found to be sufficient to cover the entire study area.



Fig.1: Study area.

2 Design and execution of the survey

For data collection was enough to use two instrumental positions (Fig.2), using spherical targets, not really needed for the type of performed processing, but useful for verification and / or any other processes.

Since surveys were carried out in two different epochs, it was necessary to create a targets handling and fix the exact positions and settings of the acquisition tools.

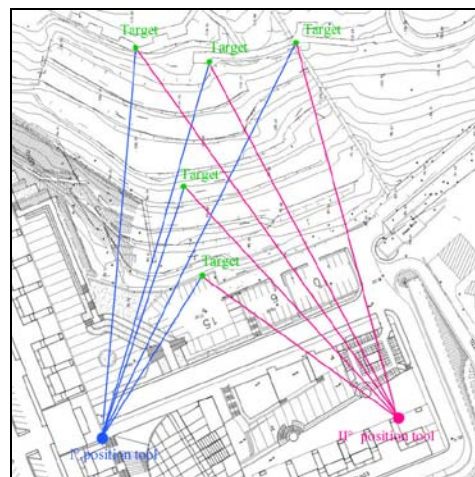


Fig.2: Survey area and shooting design.

3 First method

As first method we used the algorithm ICP (Iterative Closest Point).

3.1 Scan registration

After acquiring data set in the test site, the first operation carried out in the laboratory was the recording of different scans.



(a)



(b)

Fig.3: Point cloud after registration at t_1 and t_2 ages.

It made possible to generate a unique point cloud representing the investigated object (Fig.3 a, b).

To record the clouds and generate the whole cloud, each time was used the ICP algorithm (Iterative Closest Point) [1] implemented in the MatLab environment.

The ICP algorithm iteratively applied a rigid roto-

translation in one of the two clouds, considered to be mobile, so that overlap in the best possible way to another cloud, considered fixed.

Given a point cloud V^j and a point cloud V^i to align with each other, for each y_i point of V^j , exists at least one x_i point on the cloud V^i , said corresponding point, which is the closest to y_i compared to all other points in X .

The algorithm is an efficient method to tackle rigid registration between two point sets. Its goal is to find a rigid transformation, with which Y is registered to be in the best alignment with X , that is, let T of Equation:

$$T, j \in \{1, 2, \dots, N_x\} \left(\sum_{i=1}^{N_y} \left\| T(\vec{y}_i) - \vec{x}_j \right\|_2^2 \right) \quad (1)$$

be rotation and translation transformations, hence the rigid registration between two point sets is

$$R, t, j \in \{1, 2, \dots, N_x\} \left(\sum_{i=1}^{N_y} \left\| (R\vec{y}_i + t) - \vec{x}_j \right\|_2^2 \right) \quad (2)$$

$$\text{s.t. } R^T R = I_x; \det(R) = 1$$

In an iteration, ICP assumes that the closest points correspond, computes the absolute orientation and applies the resulting rigid transformation to V^j . In practice, at step 1 for each point of mobile cloud (V^j set), are sought, within the fixed point cloud, the points (closest point) contained in a sphere of a certain radius (multiple of a parameter introduced by user) belonging to V^i set. The closest of these will be held and considered the corresponding point.

$$C_k(i) = \arg \min_{j \in \{1, 2, \dots, N_x\}} \left(\left\| (R_{k-1}\vec{y}_i + t_{k-1}) - \vec{x}_j \right\|_2^2 \right) \quad (3)$$

With these matches found, in step 2, the algorithm computes the incremental transformation (rotation matrix $R_{i,j}$ and translation vector T and solving the absolute orientation) by applying it to the elements of V^j ; if the mean square error is less than a certain threshold, the iteration terminates otherwise return to step 1;

$$(R_k, t_k) = \arg \min_{R^T R = I_m, \det(R) = 1, t} \left(\left\| (R\vec{y}_i + t) - \vec{x}_{C_k(i)} \right\|_2^2 \right) \quad (4)$$

The principle on which is based this algorithm is

that the alignment between the two point clouds corresponds to the minimization of the quadratic error of the minimum distances between the two objects. In fact, Besl and McKay demonstrated that the algorithm converges to a local minimum of the error (Fig.4).

$$e = \sum_{i=1}^N \|x_i - (R_{y_i} - T)\|^2 = \min \quad (5)$$

$$C: V^j \rightarrow \frac{V^i}{\forall y} \in V^j \exists x \text{ such that } \min \text{ distance } (y, x) < \sigma \quad (6)$$

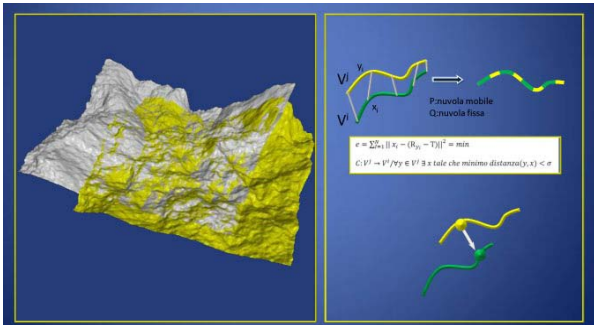


Fig.4: Iterative closest point.

3.2 Subsequent processing

Completed the registration steps, cleaning and filtering, repeated for two epochs that characterize the methodology tested, and in order to delimit the areas of interest and eliminate the present vegetation, we proceed to the generation of DEM, segmenting the entire point cloud in small regions 2.5 D (Fig.5 and Fig.6).

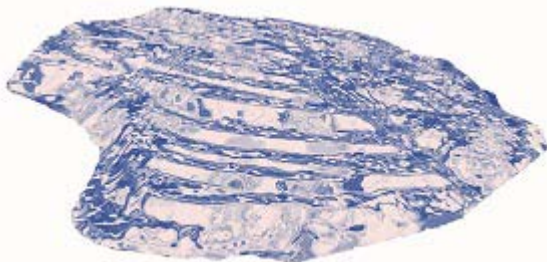


Fig.5: DEM created after segmentation of new cloud at t_1 age.

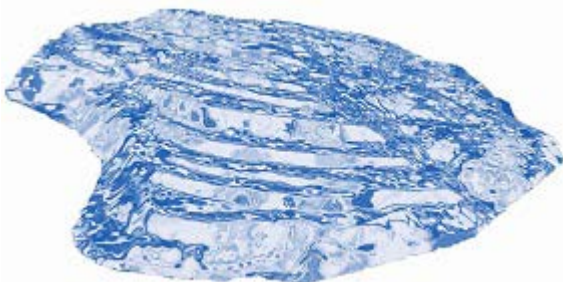


Fig.6: DEM created after segmentation of new cloud at t_2 age.

For this purpose was used the Ransac (Random Sample Consensus) algorithm [2] with a voxel approach that generates a pyramidal structure from which are extracted flat elements. These plans were subsequently aggregates, using a hierarchical clustering, to build a single plane of greater dimensions.

Thus transforming the point cloud of all ages in DEM [3] in the form of a square grid of δ DEM resolution, proceed with the analysis of the Δ DEM differences between the two epochs t_1 and t_2 .

However, from previous experience with the segmentation of LIDAR data, and because of the amount of data from scans with TLS, it would be impossible enter all points on the algorithm [4].

From the cloud are filled levels of the pyramid. At each level, from bottom to top, the surface of the soil is simplified by reducing the number of points (“smoothing”).

This is done with a “voxel”, enclosing the point cloud in a box (Table 1).

The generation of the pyramid starts from the lowest level, where the cells have smaller size. The points corresponding to each cell are replaced by their center of gravity. From one level to the next, 8 cells of lower level are grouped in a new cell of the upper layer. The point associated with the cell becomes the center of gravity of the 8 mothers cells. This leads to a reduction factor of 4 for each level. Then the problem becomes more computationally easy, as seen in others applicative fields [5] [6].

LVL No.	Points No.	Avg. dist (cm)	STD (cm)	Planes No.
0	2,700,000	0.0	0.0	1117
1	1,345,000	2.3	4.8	805
2	430,632	4.3	5.0	496
3	257,389	7.9	15.0	376

Table 1: Plans extracted in each level of the pyramid.

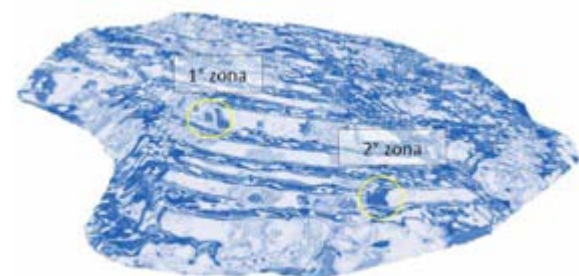


Fig.7: DEM and chosen plans of deformation control.

From the data of the segmentation, and the relative plans, two zones (Fig.7) are chosen for the control of the deformations: a well in reinforced concrete and a zone with exposed rock.

The algorithm of deformation analysis uses some parameters regulating research (Table 2). First, the size of the average window (W_{def}) defines the range within which to calculate the deformation on ΔDEM . The individual average windows are spaced by an interval Δw .

$\delta w(r,s)$ is the deformation and $\sigma_{\delta w}$ its s.q.m the value of which will be much lower, the greater will be the ability to detect even small deformations.

For discriminating whether the average $\delta w(r,s)$ of the displacements within each window represents or does not represent a significant value, there will be a statistical test.

In particular, since the parameter $\delta w(r,s)$ is the average of a sample of data that, for now, are considered independent from each other, we test the hypothesis $H_0: \delta w=0$. If the null hypothesis will be tested, the displacement δw will not be considered significant. Otherwise, the alternative hypothesis matches the significance of the deformation within the window. The statistical analysis used for the test is the following:

$$\xi = \frac{\delta_w}{\sigma_{\delta w}} \approx N(0,1) \tag{7}$$

Set a given level of risk α and its corresponding critical value $\xi_{\alpha/2}$, H_0 is rejected if $|\xi| > \xi_{\alpha/2}$.

It is therefore possible to set a minimum threshold for accepting the significance of a deformation as:

$$\delta_{wdef} = \sigma_{\delta w} \cdot \xi_{\alpha/2} \tag{8}$$

parameters	Zone 1 (cockpit in reinforced concrete)		Zone 2 (exposed rock)	
	cm	DU	cm	DU
W_{def}	35	7	35	7
Δw	5	1	5	1
$\eta(\%)$	95	95	90	90
$\sigma_{\delta w}$	± 0.05	± 0.01	± 0.05	± 0.01
δ_{wdef}	± 0.5	± 0.1	± 0.5	± 0.1

Table 2: Thresholds of the input process.

In Fig.8 we can assess, with a false-color scale, the displacements in the two areas (cockpit and rock).

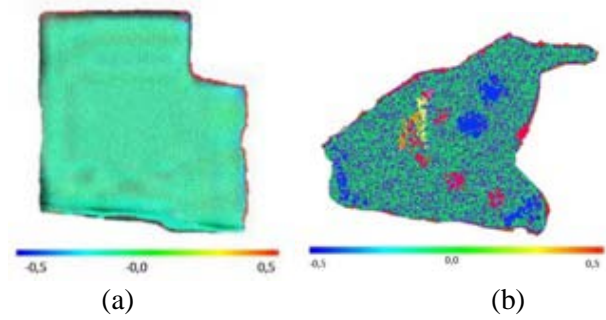


Fig.8: Well (a) and exposed (b) rock deformations.

4 Second method

As second method we used the algorithm “Least squares 3D surface matching” (Fig.9).

4.1 Scan registration

The first operation performed after the take-over phase was therefore recording different scans with a procedure based on the algorithm of “Least Squares 3D surface matching” [7] without the need of using targets in data processing, however, present during scanning.

The recording of the entire cloud at each epoch is done so by applying a global matching. The mathematical model used considers the reflection that, at every point of the first surface $f_{(x,y,z)}$ has an exact match with $g_{(x,y,z)}$ and with $e_{(x,y,z)}$ the error vector (random errors).

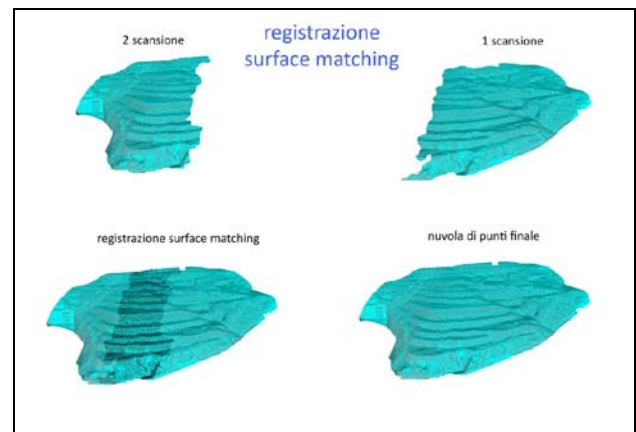


Fig.9: Schematization of the surface matching with LS3D.

The matching is obtained by the least squares objective function that represents the sum of squared Euclidean distances between the two surfaces (Table 3, Table 4).

$$\sum \left\| \vec{d} \right\|^2 = \min \tag{9}$$

No	TMP scan no (#)	SRC scan n (#)	No.of TMP points (K)	No.of SRC points (K)	No. of COR points (K)	Inter.	Time (sec)	Sigma naught (cm)
1	1	2	2063	2008	1376	3	1324	0,3

Table 3: Numerical results of the “surface matching” LS3D with the two clouds of point at the time t_1 .



Fig.10: Global cloud of points cleaned after the recording with LS3D of the scan at the time t_1 .

No	TMP scan no (#)	SRC scan n (#)	No.of TMP points (K)	No.of SRC points (K)	No. of COR points (K)	Inter.	Time (sec)	Sigma naught (cm)
1	1	2	1978	2043	1412	3	1342	0,3

Table 4: Numerical results of the “surface matching” LS3D with the two clouds of point at the time t_2 .

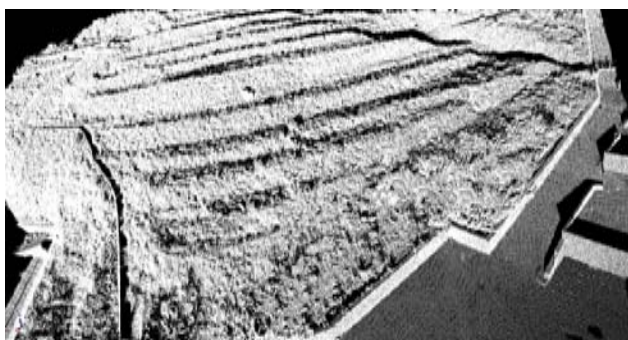


Fig.11: Global cloud of points cleaned after the recording with LS3D of the scan at the time t_2 .

4.2 Subsequent control of deformation

Once registered scans for the generation of clouds at two times t_1 (Fig.10) and t_2 (Fig.11), the “global

matching” is re-applied to monitor the deformation [8].

The procedure involves three steps:

1. global matching of the two point clouds over the area selected as stable;
2. global matching of all points of the clouds over an area already found stable and searching for areas of possible movement;
3. local matching of selected areas to estimate the deformation.

In the first step the algorithm LS3D is applied to areas that we assume as stable (Fig.12), eliminating areas with possible movements; the two clouds (registered) to the two epochs are traced thus in a common reference system (Table 5)..



Fig.12: Stable area chosen for “global matching”.

No	TMP scan no (#)	SRC scan n (#)	No.of TMP points (K)	No.of SRC points (K)	No. of COR points (K)	Inter.	Time (sec)	Sigma naught (cm)
1	1	2	487	486	486	2	303	0,3

Table 5: Numerical results of the “global matching” of the clouds of point at the time t_1 and t_2

The second step is based on the same matching technique, but drawing the two point clouds, already traced in the same reference system, and considering whole clouds, therefore not only stable areas but also the areas (Fig.13) with possible movements (Table 6).

No	TMP scan no (#)	SRC scan n (#)	No.of TMP points (K)	No.of SRC points (K)	No. of COR points (K)	Inter.	Time (sec)	Sigma naught (cm)
1	1	2	2695	2609	2543	3	1793	0,25

Table 6: “Global matching” considering the stable areas and those with possible movements

The last stage of the method consists in the

estimation of relative movement to some portions of the hill using the same method but using LS3D local matches in a "local matching" [9] [10]. Selected portions for analysis, for each "patch" on the cloud at the time t_1 is automatically detected by the subset corresponding LS3D the cloud at the time t_2 , thus obtaining the seven transformation parameters that describe the deformation and, in particular, the three translations and the three rotations (Table 7).



Fig.13: The areas chosen for the control of the deformations.

Deformation parameters	Unit	Cockpit	Rock
t_x	cm	0,11	0,32
t_y	cm	0,32	0,29
t_z	cm	-0,26	-0,52
ω	gon	0,2	0,1
φ	gon	0,1	0,05
κ	gon	0,09	0,07
m	Pure number	1	1

Table 7: Results of monitoring of deformations in the two regions examined with LS3D (shifts measured in centimeters and rotations in gons (1 circle 400gons)).

5 Conclusion

The ICP algorithm adopts a model-data concept and employs one-way correspondence.

A similar one-way correspondence approach can be found in the Least Squares 3D Surface Matching (LS3D) method that extended the least squares image matching algorithm to incorporate the 3D geometry of point clouds. The LS3D method maintained the fundamental least squares image matching concept of a template dataset and search dataset. The mathematical formulation involves the

correspondences between points from the template dataset and local planes from the search dataset.

The ICP, and in general all surface registration methods, require heavy computations. Another lack of the ICP method is to be not able to handle multiscale range data. The 3D surface matching technique, that is a generalization of the least squares 2D image matching concept, offers high flexibility for any kind of 3D surface correspondence problem, as well as monitoring capabilities for the analysis of the quality of the final results by means of precision and reliability criterions, with the ability to handle multi-resolution, multi-temporal, multiscale, and multi-sensor data sets.

The experience carried out has highlighted the benefits of both methodologies: particularly the use of the ICP algorithm, which does not need in the phase of record of the scansions of the use of targets, has supplied of the appreciable results allowing to obtain results comparable with the classic methods.

The latters instead need of homologues targets for the generation of the whole point cloud. ICP algorithm might be fundamental where, because of the possible deformations, the monumentation of the targets might not guarantee the certainty of the obtained datum, distorting the results and checks to be achieved.

The benefits of LS3D instead they are, to exploit all the information provided by the geometry of the 3D cloud of points to be able to measure strain with a magnitude less than the accuracy of the instrument. Also is to implement a flexible procedure that can be applied with any type of scenes including a wide range of applications of deformation and allows to measure movement in three dimensions, not only along a preferred direction [11] [12].

The use of Laser Scanner can make an important contribution to the analysis of the deformation due to landslides. The two procedures gave comparable deformation values.

References:

- [1] C.A. Kapoutsis, C. P. Vavoulidis, I. Pitas. Morphological iterative closest point algorithm, *IEEE Transactions on Image Processing*, Vol.8, No.11, 1999.
- [2] R. W. Schnabel, R. Klein, Ransac Based Out-of-Core Point-Cloud Shape Detection for City-Modeling, *Proceedings of Terrestrisches*

- Laserscanning* (TLS 2007), Beiträge zum 74. DVW Seminar, Fulda, Germany, 2007.
- [3] R. Lindenbergh, N. Pfeifer, A statistical deformation analysis of two epochs of terrestrial laser data of a lock, *Proceedings of 7th Conference on Optical 3-D Measurement Techniques*, Austria, 3–5 October 2005, Vol. 2, pp. 61-70.
- [4] A. Abellán, M. Jaboyedoff, T. Oppikofer, J. Vilaplana, Detection of millimetric deformation using a terrestrial laser scanner: experiment and application to a rockfall event, *Natural Hazards and Earth System Sciences*, Vol.9, 2009, 365-372.
- [5] V. Barrile, G. M. Meduri, G. Bilotta, Laser scanner surveying techniques aiming to the study and the spreading of recent architectural structures, *Recent advances in signals and systems, Proceedings of the 9th WSEAS International Conference on Signal, speech and image processing*, 2009, pp. 92-95.
- [6] V. Barrile, G. M. Meduri, G. Bilotta, Laser scanner technology for complex surveying structures, *WSEAS transactions on signal processing*, Vol.7, No.3, 2011, pp. 65-74.
- [7] P.J. Besl, N.D. McKay, A method for registration of 3-D shapes, *IEEE Transactions on Pattern Analysis and Machine Intelligence*, Vol.14, No.2, 1992, pp. 239-256.
- [8] A. Gruen, D. Akca, Least squares 3D surface and curve matching, *ISPRS Journal of Photogrammetry and Remote Sensing*, Vol.59, No.3, 2005, pp. 151-174.
- [9] J. Gomes Mota, *Localisation of Mobile Robots using Scanned Laser and Reconstructed 3D Models*, MSc Thesis, Instituto Superior Técnico, Universidade Técnica de Lisboa, Portugal, May 2002.
- [10] S.J. Gordon, D.D. Lichti, Terrestrial laser scanners with a narrow field of view: the effect on 3D resection solutions, *Survey Review*, Vol.37, No.292, 2004, pp. 448-468.
- [11] V. Barrile, G. Bilotta, G. M. Meduri, Least Squares 3D Algorithm for the Study of Deformations with Terrestrial Laser Scanner, in *Recent Advances in Electronics, Signal Processing and Communication Systems, Proceedings EUROPMENT 2013 International Conference on Electronics, Signal Processing and Communication Systems*, ESPCO 2013, Venice, Italy, Sept. 28-30, 2013, pp. 162-165.
- [12] V. Barrile, G. Bilotta, G. M. Meduri, An application of the Least Squares 3D algorithm for territorial monitoring and control, *International Journal of Systems Applications, Engineering & Development*, Vol.8, 2014, pp. 18-25.